



# A bright red-emitting flavonoid for Al<sup>3+</sup> detection in live cells without quenching ICT fluorescence†

Cite this: *Chem. Commun.*, 2019, 55, 7041

Chathura S. Abeywickrama,<sup>a</sup> Keti A. Bertman<sup>a</sup> and Yi Pang<sup>ib</sup> \*<sup>ab</sup>

Received 25th March 2019,  
Accepted 22nd May 2019

DOI: 10.1039/c9cc02322d

rsc.li/chemcomm

**A bright red-emitting flavonoid derivative was synthesized, which exhibited a large Stokes shift ( $\Delta\lambda > 150$  nm) and high fluorescence quantum yields ( $\phi_f = 0.10$ – $0.35$ ). The probe could form a stable complex with Al<sup>3+</sup> in 1:1 binding stoichiometry, generating a large bathochromic shift in both absorption and fluorescence ( $\Delta\lambda \approx 70$  nm) to enable ratiometric determination of cellular Al<sup>3+</sup>.**

As the most abundant metal in the earth's crust, aluminium-based products are widely used in household products (*e.g.* cooking wares) and constructions materials.<sup>1,2</sup> However, a high concentration of Al<sup>3+</sup> is toxic to living organisms due to its potential neurotoxicity.<sup>3–5</sup> Increased Al<sup>3+</sup> levels in the human body can lead to severe disease conditions such as dementia, Alzheimer's disease, Parkinson's disease, Al-related bone diseases (ARBD), encephalopathy, and myopathy.<sup>6–11</sup> Therefore, monitoring Al<sup>3+</sup> level in the human body will be useful in identifying potential risk of such disease conditions. According to recent World Health Organization (WHO) reports, the recommended daily Al<sup>3+</sup> intake is 3–10 mg per day, whereas the recommended Al<sup>3+</sup> concentration level in drinking water is below 200  $\mu\text{g L}^{-1}$ .<sup>12,13</sup> Therefore, the development of highly sensitive and reliable techniques for the detection of Al<sup>3+</sup> level is essential in biological research. Atomic absorption spectroscopy, mass spectrometry, voltammetry, ion selective membranes and liquid chromatography coupled mass spectrometry are commonly used for detecting Al<sup>3+</sup> ions in aqueous solutions.<sup>14–17</sup> However, these methods are not suitable for cellular studies.

Fluorescent sensors for Al<sup>3+</sup> detection in an aqueous environment have gained more attention recently, due to their high sensitivity and selectivity.<sup>18–24</sup> However, the most challenging step is to identify a suitable ligand for Al<sup>3+</sup> binding, due to

the strong hydration of the Al<sup>3+</sup> cation.<sup>18</sup> The current designs of fluorescent Al<sup>3+</sup> probes utilize chelating groups such as hydrazides, Schiff bases, urea/thiourea conjugates and pyrene–amino acid conjugates for Al<sup>3+</sup> binding. However, the currently reported Al<sup>3+</sup> probes suffer from major drawbacks, including their characteristic blue emission, small Stokes shifts, poor chemical stability in aqueous environments, low biocompatibility and higher energy excitation, which limit their applications in biological environments.<sup>18–21,25–30</sup> Therefore, it is desirable to develop red-emitting, highly biocompatible probes with large Stokes shifts for bio-imaging applications.

Flavonoids are a class of naturally occurring dyes, which often exhibit beneficial biological properties and find uses as anti-oxidants,<sup>31–35</sup> anti-inflammatory agents,<sup>35,36</sup> anti-microbial drugs,<sup>33,37</sup> and anti-cancer drugs.<sup>38–42</sup> Due to their low toxicity and environmentally sensitive fluorescence with a large Stokes shift ( $\Delta\lambda \approx 100$ – $150$  nm),<sup>43</sup> flavonoids have been used in the design of fluorescent chemical sensors for proteins,<sup>44</sup> cations,<sup>45</sup> and other biological imaging applications.<sup>44,46,47</sup> However, the existing flavonoid probes have limited conjugation, which typically show fluorescence in the blue and green region, since many of them are based on the structure of **1**. In order to overcome this barrier, we now report the synthesis of flavonoid derivative **2**, in which a vinyl bond is inserted between the B and C rings for extended conjugation and intramolecular charge transfer (ICT) interaction. The result showed that the strategy effectively shifted the  $\lambda_{\text{abs}}$  and  $\lambda_{\text{em}}$  of **2** to a longer wavelength, giving bright red-emission ( $\lambda_{\text{em}} \approx 610$  nm in EtOH) with a large Stokes shift ( $\Delta\lambda \approx 150$  nm) (Scheme 1). In addition, **2** also exhibited a large spectral response upon binding with Al<sup>3+</sup> in aqueous environments, showing its potential in detecting Al<sup>3+</sup> in biological environments.

Flavonoid derivative **2** was synthesized according to the previously reported procedure<sup>47</sup> in good yield (Scheme 1) and characterized by <sup>1</sup>H NMR and <sup>13</sup>C NMR spectroscopy, melting point determination and high-resolution mass spectrometry (ESI,† Fig. S1 and S2).

*Spectroscopic properties.* The spectroscopic properties of **2** were examined in different solvents (Table 1 and ESI,† Fig. S3).

<sup>a</sup> Department of Chemistry, University of Akron, Akron, Ohio 44325, USA.

E-mail: yip5@uakron.edu

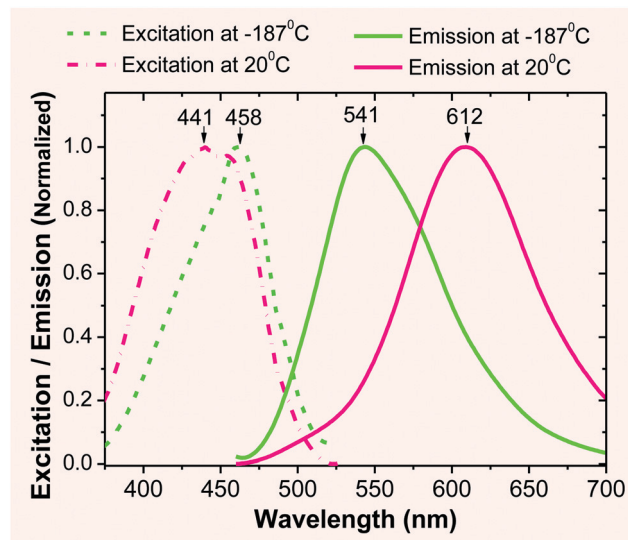
<sup>b</sup> Maurice Morton Institute of Polymer Science, University of Akron, Akron, Ohio 44325, USA

† Electronic supplementary information (ESI) available. See DOI: 10.1039/c9cc02322d

Scheme 1 Synthesis of probe **2** and the ESIPT/ICT process in probe **2**.Table 1 Spectroscopic properties of probe **2**

| Solvent      | $\lambda_{\text{abs}}$ (nm) | $\lambda_{\text{em}}$ (nm) | $\phi_{\text{fl}}$ | $\Delta\lambda$ (cm <sup>-1</sup> ) | $\Delta\lambda$ (nm) | $\epsilon$ (M <sup>-1</sup> cm <sup>-1</sup> ) |
|--------------|-----------------------------|----------------------------|--------------------|-------------------------------------|----------------------|--|
| Toluene      | 437                         | 528                        | 0.11               | 3944                                | 91                   | 27 260   |
| DCM          | 440                         | 567                        | 0.14               | 5091                                | 127                  | 28 235   |
| Acetonitrile | 432                         | 588                        | 0.37               | 6141                                | 156                  | 26 100   |
| THF          | 431                         | 561                        | 0.21               | 5377                                | 130                  | 24 395   |
| DMSO         | 444                         | 595                        | 0.33               | 5716                                | 151                  | 28 543   |
| DMF          | 438                         | 589                        | 0.32               | 5853                                | 151                  | 29 173   |
| EtOH         | 438                         | 613                        | 0.24               | 6518                                | 175                  | 29 460   |
| MeOH         | 439                         | 621                        | 0.24               | 6676                                | 182                  | 27 316   |
| Water        | 430                         | 640                        | 0.008              | 7631                                | 210                  | 16 306   |

The absorption  $\lambda_{\text{abs}}$  of **2** was affected slightly by solvent polarity ( $\Delta\lambda \approx 14$  nm, Table 1 and ESI,† Fig. S3), in sharp contrast to **1** whose absorption  $\lambda_{\text{abs}}$  was affected by  $\Delta\lambda \approx 45$  nm.<sup>47</sup> However, the emission spectra of **2** displayed a large solvatochromic effect, with emission  $\lambda_{\text{em}}$  shifting from 528 nm (in toluene) to 640 nm (in water). This can be explained by the relative stability of the polar ICT-transition state complex of probe **2** in different solvents. On the basis of the observed large Stokes shift (*e.g.*  $\Delta\lambda \approx 175$  nm in EtOH), the emission was assumed to arise from the ESIPT process that was coupled with ICT (Scheme 2). Interestingly, the emission of **2** was very weak in aqueous solutions ( $\phi_{\text{fl}} = 0.008$ ) but became strong in non-aqueous solutions ( $\phi_{\text{fl}} \approx 0.34$  in acetonitrile). Therefore, probe **2**

Scheme 2 Proposed formation of the Al<sup>3+</sup> complex with **2**. Structure **3** shows enhanced ICT in the complex.Fig. 1 Excitation (broken line) and fluorescence (solid line) spectra of **2** ( $1 \times 10^{-6}$  M) in EtOH at different temperatures.

retained the valuable environmentally sensitive fluorescence of **1**, while extending the emission to a longer wavelength.

**Low temperature fluorescence.** In order to evaluate the extent of the ICT effect, a sample of **2** (in EtOH) was frozen quickly by immersing it into liquid nitrogen in a quartz Dewar. At an extremely low temperature (*i.e.*,  $-189$  °C), the molecule of **2** was frozen in a rigid solvent matrix (*m.p.* of EtOH:  $-112$  °C), which restricted the molecular motion and bond changes that are associated with the ESIPT/ICT process. As a consequence, the emission  $\lambda_{\text{em}}$  was observed at 541 nm (Fig. 1), which could be attributed to its locally excited state. When the temperature was increased to room temperature, the emission peak was red-shifted towards 612 nm, as molecular motion became possible, enabling the ESIPT/ICT process. The observed large spectral shift ( $\Delta\lambda_{\text{em}} \approx 70$  nm from 541 nm to  $\sim 612$  nm) provided experimental evidence, supporting the assumption that the ESIPT/ICT process played an important role in the emission of **2** occurring at a longer wavelength.

**Al<sup>3+</sup> sensing in solution.** When the solution of **2** (in acetonitrile) was titrated with an Al<sup>3+</sup> (1 mM in aqueous) solution, a new absorption band was observed at  $\sim 507$  nm, whose intensity gradually increased with the Al<sup>3+</sup> concentration (Fig. 2a). The absorbance at 507 nm exhibited a good linear correlation with the Al<sup>3+</sup> concentration up to 1 equivalent. Probe **2** was excited at either 430 nm or 507 nm to record the emission spectra of the resulting Al<sup>3+</sup> complex. When **2** was excited at 430 nm, the emission peak at 588 nm gradually decreased with increasing Al<sup>3+</sup> concentration (ESI,† Fig. S4). However, excitation at 507 nm revealed the emission only from the resulting Al<sup>3+</sup> complex ( $\lambda_{\text{em}} \approx 658$  nm), which gradually increased with the Al<sup>3+</sup> concentration (Fig. 2b). The emission spectra remained unchanged after the addition of 1 equivalent of Al<sup>3+</sup> cation, indicating 1:1 binding stoichiometry for the probe 2-Al<sup>3+</sup> complex. The 1:1 ligand-to-metal ratio for the Al<sup>3+</sup> complex was determined by Job's plot (ESI,† Fig. S8). Also, the



Fig. 2 Absorption (a) and emission (b) spectra recorded for probe **2** ( $1 \times 10^{-5}$  M) in acetonitrile upon spectrometric titration with Al<sup>3+</sup> (1 mM in water) at room temperature. The **2-Al** complex was excited at 507 nm to obtain the emission spectra.

limit of detection (LOD) for probe **2** was found to be 0.05  $\mu$ M. The calculated binding constant ( $\log K$ ) for the **2-Al** complex was found to be 6.77, which further revealed the stronger binding properties of the **2-Al** complex (ESI,† Fig. S9).

The spectral evidence clearly indicated that the chelation of ligand **2** with the Al<sup>3+</sup> cation was sufficiently strong to replace the water on the metal cation, forming the **2-Al** complex. When the concentration of Al<sup>3+</sup> was less than 0.5 equiv., the equilibrium could also include some **2-Al-2**, in addition to the major product **2-Al** complex. This assumption could account for the higher response in the absorbance in the presence of 0–0.5 equiv. of Al<sup>3+</sup> (inset in Fig. 2a). Since Al<sup>3+</sup> was more reactive compared to **2-Al** (bearing two positive charge), the reaction of “**2-Al-2** + Al<sup>3+</sup> → **2** (**2-Al**)” occurred when the concentration of the Al<sup>3+</sup> cation was higher than 0.5 equiv., as the Job plot shows. This assumption also explained the lack of an ideal isobestic point in the absorption spectra (Fig. 2a). However, the fluorescence response of **2** at 658 nm was almost linear (inset in Fig. 2b). The ability of **2** to show a large spectral shift upon binding to Al<sup>3+</sup> makes it a



Fig. 3 <sup>1</sup>H NMR spectra of probe **2** in the absence (bottom) and presence (top) of one equiv. of Al<sup>3+</sup> (prepared from Al(NO<sub>3</sub>)<sub>3</sub>·9H<sub>2</sub>O dissolved in acetonitrile-*d*<sub>3</sub>) in deuterated DMSO-*d*<sub>6</sub>.

potentially useful method for ratiometric determination ( $I_{658}/I_{588}$ ) of the Al<sup>3+</sup> concentration in the solution (ESI,† Fig. S6 and S7).

The proposed formation for Al<sup>3+</sup> binding was further studied by NMR spectroscopic analysis in deuterated DMSO (Fig. 3). Addition of Al<sup>3+</sup> (1 eq.) into probe **2** resulted in the disappearance of the -OH proton signal (H<sub>a</sub>) at 9.34 ppm, which is in agreement with the proposed formation of the **2-Al** complex (Scheme 2). The aromatic proton H<sub>c</sub> signal (on the B ring of **2**) at 6.75 ppm disappeared and shifted notably downfield, indicating that ligand **2** was binding to the cation when one equiv. of Al<sup>3+</sup> was used. The noticeable downfield shift in the <sup>1</sup>H NMR signal also indicated the reduced electron density on the B ring of **2**, which is in agreement with the enhanced ICT interaction upon Al<sup>3+</sup> binding (shown in **3** in Scheme 2).

Probe **2** was tested against other cationic species to investigate its selective interaction with metal cations. Interestingly, **2** did not show any noticeable optical response towards any other cationic species except for Al<sup>3+</sup> (ESI,† Fig. S11). Therefore, it could be used for selective identification of Al<sup>3+</sup> in the presence of other metal ion species.

**Al<sup>3+</sup> detection in live cells.** The attractive photophysical properties, in addition to its selectivity towards Al<sup>3+</sup>, led us to investigate the potential use of **2** for Al<sup>3+</sup> detection in live cells. Thus, progenitor oligodendrocytes (MO3.13) were pre-incubated with an aqueous Al<sup>3+</sup> solution (1  $\mu$ M) for 30 minutes and then incubated with probe **2** (1  $\mu$ M) for another 30 minute period. As a control experiment, another batch of MO3.13 cells was incubated with probe **2** (1  $\mu$ M) in the absence of Al<sup>3+</sup> in the media. Surprisingly, the cells pre-incubated with Al<sup>3+</sup> showed bright red fluorescence confocal images upon exciting probe **2** with a 561 nm laser line (Fig. 4c and d). In sharp contrast, the cells incubated with probe **2** (1  $\mu$ M) only (*i.e.*, absence of Al<sup>3+</sup>) did not reveal any noticeable fluorescence signal (Fig. 4a and b) upon 561 nm laser excitation. However, probe **2** (1  $\mu$ M) showed weak red emission upon excitation with a 488 nm laser (ESI,† Fig. S12). This result illustrated that probe **2** could be a reliable tool for determination of Al<sup>3+</sup> toxicity in live cells. It is also important to notice that the probe showed bright confocal microscopy images with Al<sup>3+</sup> concentrations as low as 1  $\mu$ M, which is a



Fig. 4 Fluorescence confocal microscopy images of the MO3.13 cells stained with probe 2 (1  $\mu\text{M}$ ) for 30 minutes at 60 $\times$  oil magnification. Images (a) and (b) represent the control experiment carried out in the absence of  $\text{Al}^{3+}$  in the media. Images (c) and (d) represent the cells pre-incubated with a 1  $\mu\text{M}$  solution of  $\text{Al}^{3+}$  for 30 minutes before introducing probe 2. The cells were excited using a 561 nm laser line and the emission was recorded in the 580–700 nm range.

significant improvement in comparison to previously reported  $\text{Al}^{3+}$  sensing fluorescent probes.

In conclusion, flavonoid derivative 2 was synthesized in good yield, which exhibited excellent selectivity towards  $\text{Al}^{3+}$ . Probe 2 exhibited a large Stokes shift ( $\Delta\lambda > 150$  nm) due to  $\text{Al}^{3+}$  binding enhanced ICT. Bright red emission ( $\lambda_{\text{em}} \approx 640$  nm) could be generated upon binding with  $\text{Al}^{3+}$  due to the formation of the 2-Al complex, with a 1 : 1 ligand-to-metal ratio. Very good response towards  $\text{Al}^{3+}$ , while being silent to other metal ions, indicated that probe 2 could be a potentially useful sensor for tracking  $\text{Al}^{3+}$  concentrations in biological cells.

We acknowledge the Coleman endowment from the University of Akron. We also thank Dr Leah Shriver from the University of Akron for the generous gift of the MO3.13 cell line, Dr Michael Konopka from the University of Akron for assistance in bio-imaging, and Nicolas Alexander for providing mass spectrometry data.

## Conflicts of interest

There is no conflict of interest to declare.

## References

- G. H. Robinson, *Chem. Eng. News*, 2003, **81**, 54.
- C. Exley, *J. Inorg. Biochem.*, 2005, **99**, 1747–1920.
- M. I. Yousef, A. M. A. El-Morsy and M. S. Hassan, *Toxicology*, 2005, **215**, 97–107.
- H. Bielarczyk, A. Jankowska, B. Madziar, A. Matecki, A. Michno and A. Szutowicz, *Neurochem. Int.*, 2003, **42**, 323–331.
- D. R. Burwen, S. M. Olsen, L. A. Bland, M. J. Arduino, M. H. Reid and W. R. Jarvis, *Kidney Int.*, 1995, **48**, 469–474.
- S. Goswami, S. Paul and A. Manna, *RSC Adv.*, 2013, **3**, 10639–10643.
- D. Jeyanthi, M. Iniya, K. Krishnaveni and D. Chellappa, *RSC Adv.*, 2013, **3**, 20984–20989.
- T. P. Flaten, *Brain Res. Bull.*, 2001, **55**, 187–196.
- C. N. Martyn, C. Osmond, J. A. Edwardson, D. J. P. Barker, E. C. Harris and R. F. Lacey, *Lancet*, 1989, **333**, 59–62.
- P. Nayak, *Environ. Res.*, 2002, **89**, 101–115.
- D. P. Perl, D. C. Gajdusek, R. M. Garruto, R. T. Yanagihara and C. J. Gibbs, *Science*, 1982, **217**, 1053–1055.
- Z. Krejpcio and R. W. Wojciak, *Pol. J. Environ. Stud.*, 2002, **11**, 251–254.
- J. Barcelo and C. Poschenrieder, *Environ. Exp. Bot.*, 2002, **48**, 75–92.
- M. Frankowski, A. Ziola-Frankowska and J. Siepak, *Talanta*, 2010, **80**, 2120–2126.
- A. Sanz-Medel, A. B. S. Cabezuelo, R. Milačić and T. B. Polak, *Coord. Chem. Rev.*, 2002, **228**, 373–383.
- R. N. Goyal, V. K. Gupta and S. Chatterjee, *Biosens. Bioelectron.*, 2009, **24**, 3562–3568.
- V. K. Gupta, A. K. Singh, S. Mehtab and B. Gupta, *Anal. Chim. Acta*, 2006, **566**, 5–10.
- D. Maity and T. Govindaraju, *Eur. J. Inorg. Chem.*, 2011, 5479–5485.
- K. Boonkitpatarakul, J. Wang, N. Niamnont, B. Liu, L. McDonald, Y. Pang and M. Sukwattanasinitt, *ACS Sens.*, 2015, **1**, 144–150.
- J.-C. Qin, X. Cheng, R. Fang, M. Wang, Z. Yang, T. Li and Y. Li, *Spectrochim. Acta, Part A*, 2016, **152**, 352–357.
- X. Sun, Y.-W. Wang and Y. Peng, *Org. Lett.*, 2012, **14**, 3420–3423.
- Y.-W. Wang, Y.-X. Hua, H.-H. Wu, X. Sun and Y. Peng, *Chin. Chem. Lett.*, 2017, **28**, 1994–1996.
- Y.-W. Wang, S.-B. Liu, W.-J. Ling and Y. Peng, *Chem. Commun.*, 2016, **52**, 827–830.
- T. Ma, M. Dong, Y. Dong, Y. Wang and Y. Peng, *Chem. – Eur. J.*, 2010, **16**, 10313–10318.
- L. McDonald, J. Wang, N. Alexander, H. Li, T. Liu and Y. Pang, *J. Phys. Chem. B*, 2016, **120**, 766–772.
- J. Zhang, S. Chen, Y. Ma, D. Wang, J. Zhang, Y. Wang, W. Li, Z. Yu, H. Zhang and F. Yin, *J. Mater. Chem. B*, 2018, **6**, 4065–4070.
- Q. Xia, Z. Chen, Z. Yu, L. Wang, J. Qu and R. Liu, *ACS Appl. Mater. Interfaces*, 2018, **10**, 17081–17088.
- Q. Xu, T. Kuang, Y. Liu, L. Cai, X. Peng, T. S. Sreepasad, P. Zhao, Z. Yu and N. Li, *J. Mater. Chem. B*, 2016, **4**, 7204–7219.
- P. Miao, B. Wang, Z. Yu, J. Zhao and Y. Tang, *Biosens. Bioelectron.*, 2015, **63**, 365–370.
- B. Li, H. Wen, Y. Cui, W. Zhou, G. Qian and B. Chen, *Adv. Mater.*, 2016, **28**, 8819–8860.
- Y. Zhang, D. Wang, L. Yang, D. Zhou and J. Zhang, *PLoS One*, 2014, **9**(8), e105725.
- M. G. L. Hertog, E. J. M. Feskens, D. Kromhout, M. G. L. Hertog, P. C. H. Hollman, M. G. L. Hertog and M. B. Katan, *Lancet*, 1993, **342**, 1007–1011.
- P. G. Pietta, *J. Nat. Prod.*, 2000, **63**, 1035–1042.
- P. A. Nijveldt, R. J. Van Nood, E. L. S. Van Hoorn, D. E. Boelens, P. G. Van Norren and K. Van Leeuwen, *Am. J. Clin. Nutr.*, 2001, **74**, 418–425.
- Z. Hanáková, J. Hošek, Z. Kutil, V. Temml, P. Landa, T. Vaněk, D. Schuster, S. Dall'Acqua, J. Cvačka, O. Polanský and K. Šmejkal, *J. Nat. Prod.*, 2017, **80**, 999–1006.
- H. Lim, H. Park and H. P. Kim, *Biochem. Pharmacol.*, 2015, **96**, 337–348.
- T. P. T. Cushnie and A. J. Lamb, *Int. J. Antimicrob. Agents*, 2005, **26**, 343–356.
- M. K. Chahar, N. Sharma, M. P. Dobhal and Y. C. Joshi, *Pharmacogn. Rev.*, 2011, **5**, 1–12.
- C. Faggio, A. Sureda, S. Morabito, A. Sanches-Silva, A. Mocan, S. F. Nabavi and S. M. Nabavi, *Eur. J. Pharmacol.*, 2017, **807**, 91–101.
- B. H. Havsteen, *The biochemistry and medical significance of the flavonoids*, 2002, vol. 96.
- Y. Zhang, N.-D. Yang, F. Zhou, T. Shen, T. Duan, J. Zhou, Y. Shi, X.-Q. Zhu and H.-M. Shen, *PLoS One*, 2012, **7**, e46749.
- G. Galati and P. J. O'Brien, *Free Radical Biol. Med.*, 2004, **37**, 287–303.
- A. S. Klymchenko, *Acc. Chem. Res.*, 2017, **50**, 366–375.
- B. Liu, Y. Pang, R. Bouhenni, E. Duah, S. Paruchuri and L. McDonald, *Chem. Commun.*, 2015, **51**, 11060–11063.
- C. Zhao, B. Liu, X. Bi, D. Liu, C. Pan, L. Wang and Y. Pang, *Sens. Actuators, B*, 2016, **229**, 131–137.
- L. McDonald, B. Liu, A. Taraboletti, K. Whiddon, L. P. Shriver, M. Konopka, Q. Liu and Y. Pang, *J. Mater. Chem. B*, 2016, **4**, 7902–7908.
- K. A. Bertman, C. S. Abeywickrama, H. J. Baumann, N. Alexander, L. McDonald, L. P. Shriver, M. Konopka and Y. Pang, *J. Mater. Chem. B*, 2018, **6**, 5050–5058.